ISSN 1990-7478, Biochemistry (Moscow), Supplement Series A: Membrane and Cell Biology, 2018, Vol. 12, No. 3, pp. 287–302. © Pleiades Publishing, Ltd., 2018.
Original Russian Text © A.V. Vershubskii, S.M. Nevyantsev, A.N. Tikhonov, 2018, published in Biologicheskie Membrany, 2018, Vol. 35, No. 2, pp. 87–103.

ARTICLES

Modeling of Electron and Proton Transport in Chloroplast Membranes with Regard to Thioredoxin-Dependent Activation of the Calvin–Benson Cycle and ATP Synthase

A. V. Vershubskii[a], S. M. Nevyantsev[a], and A. N. Tikhonov[a, *]

[a] *Faculty of Physics, Moscow Lomonosov State University, Moscow, 119991 Russia*

**e-mail: an_tikhonov@mail.ru*

Received June 18, 2017; in final form, July 24, 2017

Abstract—In this work, the analysis of electron and proton transport in chloroplasts of higher plants has been carried out on the basis of a mathematical model, which takes into account the pH-dependent regulation of electron transfer and thioredoxin-dependent activation of the Calvin–Benson cycle (CBC) enzymes and the ATP synthase. The impact of reduced thioredoxin on the kinetics of electron transport, pH changes in the intrathylakoid space and ATP production has been simulated. Comparison of the computed and experimental data on the kinetics of P_{700} photooxidation has shown that the consideration of thioredoxin-dependent activation of the CBC and the ATP synthase provides an adequate description of the multiphase kinetics of P_{700}^{+} induction. The dynamics of electron flow through PSI and the partitioning of electron fluxes on the acceptor site of PSI has been simulated. The model predicts that at the initial stage of the induction period the alternative pathways, cyclic electron transport around PSI and electron flow to O_2 (the Mehler reaction), play a significant role in photosynthetic electron transport chain, but their contribution attenuates upon the activation of the CBC reactions.

Keywords: photosynthesis, membranes of chloroplasts, electron and proton transport, mathematical modeling

DOI: 10.1134/S1990747818020150

INTRODUCTION

Light induced processes of oxygenic photosynthesis in higher plants take place in chloroplasts containing thylakoids, flattened membrane vesicles. A lipid bilayer is the basis of the thylakoid membrane, into which pigment-protein complexes are embedded, providing absorption of light and photochemical processes associated with charge separation in photoreaction centers and electron transport reactions. In photosynthetic systems of oxygenic type (cyanobacteria, algae and chloroplasts of higher plants), there are several polypeptide complexes embedded in the membrane: photosystem I (PSI), photosystem II (PSII), light-harvesting complexes of PSI and PSII (LHCI and LHCII), cytochrome b_6f complex, ferredoxin-NADP-reductase (FNR) and ATP synthase complex (CF_0–CF_1). In addition, there are mobile carriers of electrons – plastoquinone (PQ), plastocyanin (Pc) and ferredoxin (Fd), which provide communication between the immobile protein complexes embedded into the membrane. Primary processes of photosynthesis, occurring in photoreaction centers of PSI and PSII, include several stages: absorption of light, migration of energy of the absorbed light quanta to photoreaction centers, in which primary charge separation takes place, initiating electron transport through the electron transport chain [1–7]. Two photosystems operating "in tandem" perform the transfer of two electrons from the water molecule oxidized in PSII to $NADP^+$ – the terminal electron acceptor of PSI: $H_2O \rightarrow PSII \rightarrow PQ \rightarrow b_6f \rightarrow Pc \rightarrow PSI \rightarrow Fd \rightarrow FNR \rightarrow NADP^+$. Photoinduced transport of electrons is associated with the transmembrane transfer of protons. The resulting transthylakoid electrochemical potential difference of hydrogen ions ($\Delta\tilde{\mu}_{H^+}$) is the "driving force" for the operation of ATP synthase complex, which provides the formation of ATP molecules from ADP and inorganic phosphate (P_i) [5, 6, 8, 9]. The products of the light stage of photosynthesis (NADPH and ATP) provide the synthesis of carbohydrates in the Calvin–Benson cycle (CBC) [1].

A characteristic feature of the thylakoid membranes of chloroplasts is the predominant content of galactolipids with unsaturated fatty acid residues and the presence of a large number of β-tocopherol, as well as inhomogeneous distribution of the pigment-protein and the ATP-synthase complexes along the thylakoid membranes [10–14]. A high content of unsaturated fatty acids determines high "fluidity" of the thylakoid

membranes that may contribute to the effective diffusion of the mobile carriers of the electron transport chain in lateral and transmembrane directions [15, 16]. Also, it should be noted that the lateral migration of the protein complexes, photoinduced thylakoid swelling–contraction and high density of the thylakoid packaging in grans can affect the electron transport between PSI and PSII and induction phenomena of photosynthesis [17].

The structure and mechanisms of functioning of the photosynthetic apparatus of chloroplasts has been studied currently in detail at various levels of the structural organization [2–9]. At the same time, the issues concerning the mechanisms of photosynthesis regulation and photosynthetic apparatus interaction with other biochemical systems of the cell remain topical. The products of the light stage of photosynthesis, ATP and NADPH, are consumed mostly in the CBC. Regulation of the CBC reactions includes a set of processes at different levels of organization of the photosynthetic apparatus, which provide the optimal balance of NADPH and ATP production, depending on the lighting conditions and metabolic state of chloroplasts [18–21]. The light-induced activation of the CBC reactions involves redox-dependent processes influencing the activity of enzymes due to the reduction of the thiol groups, as well as the regulatory phenomena caused by conformation changes of enzymes, induced by the accession of metabolites or the thylakoid membrane energization [21–28]. The redox-dependent activation of key enzymes is one of the main ways of the CBC activation among the mechanisms of the CBC regulation. As early as in the 1960s–1970s it was found that the activity of four CBC enzymes is regulated by light. These enzymes are phosphoribulokinase, glyceraldehyde-3-phosphate dehydrogenase, fructose-1,6-biphosphatase and sedoheptulose-1,7-biphosphatase. These enzymes have low activity in the dark, but are activated by light. The activity of ribulose bisphosphate carboxylase (RBPC, also called RuBisCo), a key CBC enzyme, also increases under illumination due to the redox-dependent activation of a "helper", RuBisCo activase enzyme [23–25]. This protein modulates the RBPC activity by releasing firmly linked inhibitors from the RBPC active site. The RuBisCo activase activity depends on the ATP/ADP ratio and is regulated depending on the state of Fd and thioredoxin (Tr), a protein which directly affects the status of thiol groups of enzymes-targets. It is unprofitable for RuBisCo to be active in the dark, since the enzyme also catalyzes a side reaction with molecular oxygen, photorespiration. Light dependent reduction of thiol groups leads to a noticeable increase in the RuBisCo activity [25].

Two types of thioredoxins (*f* and *m*) coexist in chloroplasts, which play a central role in the redox regulation of photosynthetic processes. The main form of thioredoxin activating the CBC enzymes and the ATP synthase is Tr*f* [23]. Thioredoxin is reduced by thioredoxin-reductase, the electron donor for which serves reduced ferredoxin. Thioredoxin is a small (12–14 kDa) regulatory protein with two cysteine residues in the active center, which can be oxidized with formation of disulfide bonds. Thioredoxin is reduced by thioredoxin-reductase (TrR), which, in turn, is reduced by ferredoxin (Fd $\rightarrow$ TrR $\rightarrow$ Tr). The reduced thioredoxin (TrH_2) gives electrons to target proteins by reducing their thiol groups. The CBC enzymes of chloroplasts are activated under illumination, thereby providing rapid consumption of ATP and NADPH and accelerating the outflow of electrons from PSI. TrH_2 can also activate the ATP-synthase by reducing the –S–S– bridges in the γ-subunit of the ATP synthase complex [22].

Mathematical modeling of metabolic processes is widely used for the analysis of regulatory processes in biological systems. There are two basic approaches to the simulation of light stages of photosynthesis – deterministic, based on the description of these processes by means of systems of differential equations, and stochastic, associated with the use of Monte Carlo simulation, in which the diffusion of mobile carriers is considered as a random walk. Both are used for analysis of the kinetics of light and dark processes of photosynthesis and regulation of electron transport [29–33]. The development of adequate mathematical models may also facilitate the analysis of optimal conditions for photosynthesis.

In the previous work on the modeling of oxygenic photosynthesis it was shown, in particular, that the topological factors of the lamellar system of chloroplasts (geometry and characteristic dimensions of the thylakoids) can significantly affect the spatial distribution of pH along the thylakoid membrane and the redox state of the mobile electron carriers (plastoquinone and plastocyanin) [34–39]. Those models took into account the pH-dependent mechanisms of electron transport control in chloroplasts and in cyanobacterial cells. The photoinduced decrease in the intrathylakoid pH (pH_{in}) and the elevation of stromal pH (pH_s) is known [40, 41] to reduce the activity of PSII due to non-photochemical quenching of the excitation of chlorophyll molecules in the light-harvesting antenna and slows down the plastoquinone (PQH_2) oxidation by the cytochrome b_6f complex. On the other hand, the alkalization of the stroma contributes to the activation of the CBC enzymes and accelerates the outflow of electrons from PSI [5]. As was noted above, there are other mechanisms for redox regulation of the electron transport and ATP synthesis in chloroplasts. However, these regulatory mechanisms were not included in the previous model of regulation of photosynthetic processes.

In the present work, we have extended a model of the light-dependent stages of photosynthesis by accounting for the redox-dependent activation of the CBC and the ATP synthase. Thioredoxin, which is

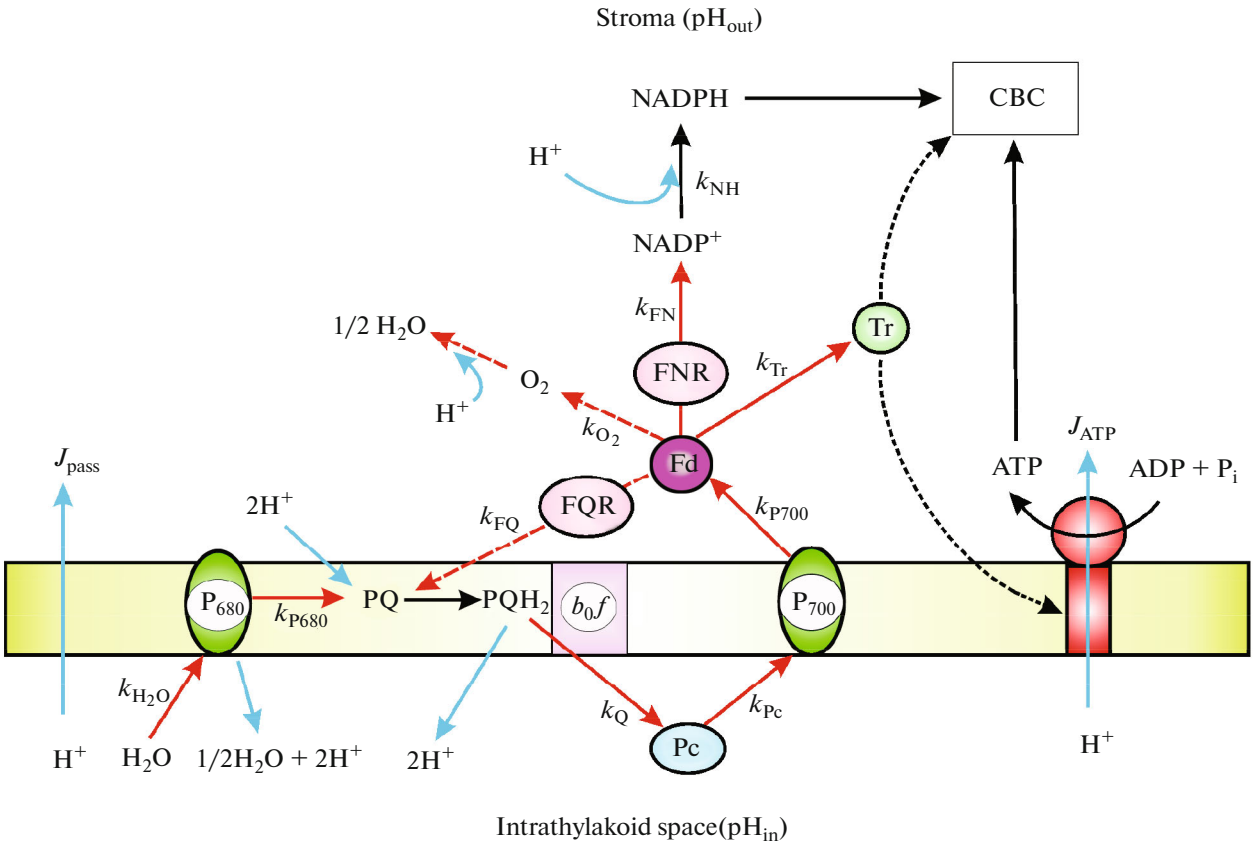

Fig. 1. The processes of electron and proton transport considered in the model. Designations: Fd, ferredoxin; Tr, thioredoxin; FNR, ferredoxin-NADP-reductase; FQR, ferredoxin-quinone reductase; P_{700} and P_{680}, primary electron donors of photosystem I (PSI) and photosystem II (PSII), respectively; Pc, plastocyanin; PQ, plastoquinone (oxidized form); PQH_2, plastoquinone (reduced form); b_6f, the cytochrome b_6f complex. Constants near the arrows indicate the rates of the corresponding reactions (the details are in the text).

reduced by thioredoxin reductase by the electrons donated by ferredoxin, is considered as the electron transfer mediator, providing the activation of the CBC and the ATP synthase. Analysis of our "numerical experiments" has shown that the consideration of mechanism of regulation allows more precise description of the features of experimentally observed multiphase P^+_{700} induction kinetics in chloroplasts in situ.

THE MODEL DESCRIPTION

For the quantitative analysis of the regulation of key stages of electron and proton transport in oxygenic type photosynthetic systems, the basic mathematical model has been used as described earlier [42–45]. The model describes the main stages of electron transfer and the coupled processes of the transmembrane transport of protons and ATP synthesis from ADP and inorganic phosphate (P_i) by the CF_0–CF_1 type ATP synthase. The scheme of the processes considered is shown in Fig. 1. It is assumed in the simulation that all the electron carriers are distributed uniformly in the thylakoid membrane and the rate of electron transfer is not diffusion-limited. This approximation is equivalent to a condition of rapid mixing. The initial system of equations, describing the behavior of the electron carriers, the change in the concentration of protons inside the thylakoid [H^+_i] and the stroma [H^+_o], the processes of evolution and consumption of molecular oxygen and the ATP concentration change in the previous model [37], which does not take into account thioredoxin-dependent activation of the Calvin–Benson cycle and the ATP synthase, is presented in the Appendix. Additional equations describing the activation of these processes by thioredoxin are shown below.

Electron transport. A complete scheme of the electron transport pathways described in the model is shown in Fig. 1. Alternative pathways of electron transport in the PSI acceptor site are considered (for details, see [44–49]). The possibility of electron transfer via alternative pathways allows for fine "tuning" of the photosynthetic apparatus, providing an optimal stoichiometry of the NADPH and ATP molecules, used in the CBC. The electron transfer from PSI to

$NADP^+$ (J_{NADP}) leads to the NADPH formation due to the electrons entering ETC from PSII (non-cyclic transport of electrons: $H_2O \rightarrow$ PSII $\rightarrow$ PSI $\rightarrow$ $NADP^+$). Ferredoxin (Fd) is the electron acceptor in PSI. Two electrons from two molecules of reduced ferredoxin (Fd^-) go to $NADP^+$ (via FNR). The cyclic electron flow around PSI (J_{SC}), in which the electrons return to the ETC between PSII and PSI through ferredoxin quinone reductase (FQR) [42], will be termed a "short" cycle. Another pathway of cyclic electron transport around PSI (J_{LC}) is possible, in principle, when electrons from NADPH are returned to the ETC between PSII and PSI via NAD(P)-oxido reductase (NDH). The contribution of this pathway is usually small due to low content of NDH in chloroplasts [50], and therefore has not been considered in this work. The third mechanism of the electron outflow from PSI is the electron transfer from PSI to O_2 molecule (the Mehler reaction) [20, 43–45]. In addition, there are terminal oxidases in chloroplasts, catalyzing the oxidation of plastquinone (PQH_2) and plastocyanin (Pc) due to the electron transfer to molecular oxygen, which are not directly related to the work of PSI and PSII. The contribution of these processes, called photorespiration, to the PQH_2 and Pc oxidation is small in comparison with the photosynthetic chain of electron transfer [51], therefore photorespiration in the description of the processes of photoinduced electron transport has been neglected. Note that relatively slow processes of photorespiraton may affect the state of ETC during the PS adaptation to the darkness that may affect the kinetics of transient processes during illumination of chloroplasts adapted to darkness [52].

The $NADP^+$ molecules reduced by PSI are protonated by hydrogen ions originating from the stroma ($NADP^+ + 2e^- + H^+ \rightarrow$ NADPH). The model takes into account that photoinduced alkalization of the stroma accelerates the NADPH and ATP consumption in the CBC. The consumption of NADPH and ATP is described phenomenologically with the help of a function, depending on the NADPH and ATP concentration and pH of the stroma (pH_o), as proposed in [37, 38].

In this work, a new variable is introduced; it is the concentration of the reduced thioredoxin ($[TrH_2]$), receiving electrons from the reduced ferredoxin (Fd^-). TrH_2 activates the redox-dependent CBC enzymes and the ATP synthase. For the phenomenological description of these processes, the system of differential equations, used in the previous works [37, 43, 44], was extended with equations describing the TrH_2 concentration change:

$$\frac{d[TrH_2]}{dt} = k_{FT}[H_o^+]\left([Fd]_0 - [Fd]\right)\left([Tr]_0 - [TrH_2]\right) - k_{Tr}^{ATP}\frac{[TrH_2]}{\eta_1 + \mu_1\left([Tr]_0 - [TrH_2]\right)} - k_{Tr}^{CBC}\frac{[TrH_2]}{\eta_2 + \mu_2\left([Tr]_0 - [TrH_2]\right)} - k_{TO}[O_2][TrH_2]. \quad (1)$$

In Eq. (1), $[TrH_2]$ is the concentration of reduced thioredoxin, [Fd] is the concentration of oxidized ferredoxin, $[O_2]$ is oxygen concentration in the medium, $[H_o^+]$ is the concentration of protons in the stroma. Equation (1) was written assuming that the rate of $[TrH_2]$ accumulation must be proportional to the concentration of the reduced ferredoxin, and its consumption is due to the interaction with thiol groups of the ATP synthase and inactive CBC enzymes. The constants k_{FT}, k_{Tr}^{ATP}, k_{Tr}^{CBC}, and k_{TO} are the effective rate constants of the corresponding reactions. The variable model parameters η_1, μ_1, η_2 and μ_2 characterize the interaction between TrH_2 with the ATP synthase and the CBC enzymes, respectively. Parameters η_1 and η_2 were supposed to be equal to 0.5 in the calculations. The constant parameters marked with subscript "0", are the maximal concentrations of the relevant variables. In formulating Eq. (1), it was assumed that thioredoxin is an enzyme which is oxidized by molecular oxygen. The first term in Eq. (1) describes the Tr reduction by Fd^-. It is possible to affect the thioredoxin redox dynamics under illumination by varying the constant k_{FT}. The last term in Eq. (1) reflects the TrH_2 oxidation rate due to its interaction with O_2; the parameter k_{TO} is an effective rate constant of the electron flow from TrH_2 to O_2.

Proton transport. Electron transport via ETC is associated with generation of the transmembrane pH difference (ΔpH). The transmembrane proton gradient is formed in thylakoids as a result of the photosynthetic proton transfer and performs an important energetic role [2–5], as well as regulatory and signaling functions [53]. Photoinduced changes of pH in the chloroplast compartments have an appreciable effect on the kinetics of electron transfer in the photosynthetic ETC, non-photochemical quenching of chlorophyll fluorescence, reversible redox transformation of xanthophylls (the so-called violaxanthin cycle), functional state of the ATP synthase and the activity of the enzymes of the dark phase of photosynthesis. The accumulation of protons inside thyilakoids occurs as a result of light-induced decomposition of water in PSII and plastoquinone (PQH_2) oxidation by cytochrome b_6f complex. The model takes into account that the hydrogen ions, localized inside (lumen) and outside (stroma) of thylakoids, may bind to proton acceptor (buffer) groups, the number of which significantly exceeds the number of the electron carriers. The influ-

ence of buffer groups has a significant impact on the kinetics of achieving the steady state of the system, but the steady state values of model variables should not depend on the buffer capacity of chloroplasts [54].

The outflow of protons from the thylakoid into the stroma can occur in two ways: through the ATP synthase (the proton flow J_{ATP} coupled with ATP synthesis) and by passive leakage of protons not associated with ATP synthesis (the proton flow J_{pass}). The model also takes into account the exchange of protons between the stroma and the cytosol (the proton flow J_{cell}). It was assumed that the concentration of hydrogen ions in the stroma $[H_o^+]$ and in the intrathylakoid space $[H_i^+]$, as well as the concentration of all electron carriers does not depend on spatial coordinates that is equivalent to the condition of "rapid mixing". The value of pH in the cytosol (the space between the chloroplast envelope and the cell membrane) is considered to be constant (pH_c 8) due to the high buffering capacity of the cytoplasm.

For the simulation of the transport of protons through the thylakoid membrane, the functions, describing the "active" and "passive" proton flows, were used, which depend on the difference of concentration of hydrogen ions $[H_i^+]$ and $[H_o^+]$. The "active" flow of protons J_{ATP} also depends on the ratio of the concentrations of ADP and ATP, the substrate and the product of the reaction catalyzed by the ATP synthase. The rationale of how the function describing the transmembrane transport of protons through the ATP synthase, as well as a description of functions and constants, which determine the flows J_{cell} and J_{pass} can be found in the previous works [37, 44]. As was mentioned above, thioredoxin may reduce the thiol groups of the ATP synthase, thereby increasing its activity. In this paper, the formula describing the proton flow through the ATP synthase has been modified by adding a multiplier $(\eta_1 + \mu_1[TrH_2])$. The modified function that describes the proton flow through the ATP synthase, coupled with synthesis of ATP is

$$J_{ATP}(t) = \frac{k_{ATP}}{m}\frac{[H_o^+][10^{\Delta pH} - 1]}{\alpha + [H_o^+][10^{\Delta pH} + \beta]}(\eta_1 + \mu_1[TrH_2]), \quad (2)$$

where k_{ATP}/m is a normalizing coefficient. Coefficients α and β in Eq. (2) are determined by pK_A of a protonated group and by the ratio of the effective rate constants k_1 and k_2: $\alpha = 10^{-pK_A}(1 + k_2/k_1)$ and $\beta = k_2/k_1$. Constants k_1 and k_2 characterize the effective rate of transfer of hydrogen ions to the protonated groups of the ATP synthesis (A^-) on the inner and outer sides of the thyilakoid membrane, respectively. Given that the acidic groups A^- of the ATP synthase rotor may be in different positions relative to the membrane *a* subunit, the values of the k_1 and k_2 constants are, generally speaking, may vary. Note that the ratio $\beta = k_2/k_1$ is a model parameter, which determines the dependence of the proton flow on the transmembrane pH difference ($\Delta pH = pH_{out} - pH_{in}$). For certain values of the parameters α and β, the J_{ATP} dependence on ΔpH has sigmoid form that reflects the threshold nature of the work of the ATP synthase (it is known that a notable ATP synthesis is observed only after exceeding a certain threshold of the proton potential [55]). It is also known that the energy threshold is reduced upon the chloroplast ATP synthase activation due to reduction of the thiol groups of the γ subunit [56]. Equation (2) takes into account the effect of activation of the ATP synthase due to the TrH_2 formation.

To describe the ATP and NADPH consumption in the CBC, a semiempirical function $k_{CBC}([ATP],[NH],[TrH_2],[H_o^+])$ was used. The detailed description of the function and justification of its choice are given in [37, 43]. The dependence of the function $k_{CBC}([ATP],[NH],[TrH_2],[H_o^+])$ on the stromal pH allows phenomenological description of the light dependent activation of the CBC reactions. To take into account the thioredoxin effect on the CBC activity, a new multiplier $(\eta_2 + \mu_2[TrH_2])$ was added to the function k_{CBC}, which allows simulation of the Tr-dependent modulation of the CBC activity. Here η_2 and μ_2 are the parameters of the model. Given the above, the NADP and ATP consumption in the CBC is described in generalized form by the following function:

$$\begin{aligned} k_{CBC}([NH],[ATP],[TrH_2]) &= \left(\frac{k^s_{min} - k^s_{max}}{1 + \exp\left\{\frac{pH_o - X_0}{\Delta X}\right\}} + k^s_{max}\right) \\ &\times \left(\frac{[ATP][NH]}{k^s_2 + k^s_3[ATP] + k^s_4[NH] + k^s_5[ATP][NH]}\right) \\ &\times (\eta_2 + \mu_2[TrH_2])\ldots \end{aligned} \quad (3)$$

The first factor in the formula is a function phenomenologically describing the pH-dependent activation of the CBC enzymes due to the photoinduced alkalization of the stroma. It was chosen according to the literature data on the CBC activation dependence on the stromal pH [1, 5].

Rate constants and the model parameters. The system of kinetic equations, describing the dynamics of the concentration changes of the electron carriers, ATP and hydrogen ions, as well as the methodology of the choice of the effective rate constants of electron-transport processes shown in Fig. 1 have been described in detail [37, 44]. The rate limiting stage of electron transfer between PSII and PSI is the PQH_2 oxidation by the cytochrome b_6f complex [49, 50]. The rate of this reaction is known to depend on the con-

centration of hydrogen ions inside the thylakoids $[H_i^+]$ [57, 58]. In the model, the rate of PQH_2 oxidation is described by the function $k_Q([PQ],[Pc],[H_i^+]) = 1/\tau_Q$, where τ_Q is the characteristic time of the PQH_2 oxidation, which is determined by the rate of PQH_2 interaction with the cytochrome b_6f complex, the time of electron transfer within the b_6f complex and the time of plastocyanin (Pc) reduction. The choice of the $k_Q([PQ],[Pc],[H_i^+])$ function was made on the basis of comparison of experimental and theoretical dependencies of the post-illumination kinetics of the P_{700}^+ reduction on the intrathylakoid pH_i (see [34, 36, 54] for details).

The values of other rate constants that characterize the different stages of electron transfer in the ETC from the water-splitting complex of PSII to various acceptors of PSI (k_{H_2O}, k_{P680}, k_{Pc}, k_{P700}, k_{FN}, k_{NH}, k_{FO}), were chosen on the basis of the literature data on the kinetics of partial reactions of electron transport in different segments of the ETC [37, 44]. The agreement of the theoretical curves with the experimental values of the electron transfer rate between PSII and PSI and intrathylakoid pH (pH_{in}) and the pH of the stromal (pH_{out}) in metabolic states 3 (the conditions of intensive ATP synthesis) and 4 (the state of photosynthetic control) were used as a criterion for the adequate choice of the rate constants. It was accepted, in particular, that, in metabolic states 3 and 4, the stationary intrathylakoid pH values were $pH_{in} \approx 6.0–6.2$ and $pH_{in} \approx 5.4– 5.6$, respectively [53, 58, 59].

RESULTS AND DISCUSSION

It is assumed that at the initial moment of time the system is considered to be in an "energy saving" mode: the CBC enzymes and the ATP synthase are inactive. It is also assumed that the initial concentrations of NADPH and TrH_2 are close to zero. At the beginning of the induction phase, when the CBC enzymes are still inactive, the Fd and NADP pools become quickly reduced. Accordingly, the flow of electrons from Fd^- to thioredoxin is increased, promoting the activation of the CBC and the ATP synthase. Below it will be considered how the inclusion of these regulatory relationships may be manifested in the kinetics of the P_{700} photooxidation. Analysis of the kinetics of P_{700} redox transients is of particular interest because the kinetics of this process can be relatively easily recorded in chloroplasts in vivo and in situ [60–64]. In the computation of the kinetic curves, the variable parameters of the model were k_{FT}, μ_1, and μ_2. The dimensionless "reference" values of these parameters in the model, from which their increase was calculated, were taken to be unity.

Figure 2 shows how the concentration of the reduced thioredoxin changes over time. The behavior of the system at different rates of electron transfer from Fd^- to thioredoxin specified by the k_{FT} constant (curves *1–3*) was considered. A sharp rise of $[TrH_2]$ was due to the fact that, at the beginning, when the outflow of electrons from Fd^- in the CBC is limited because of the low activity of the CBC enzymes, a significant portion of electrons goes from Fd^- to thioredoxin. At the same time, TrH_2 starts the activation of the CBC enzymes and the ATP synthase, resulting in accelerated consumption of NADPH. The main electron transport flow (PSI → Fd → NADP → CBC) increases, and the TrH_2 concentration decreases (Fig. 2).

Figure 3 shows the calculated curves, demonstrating how the activation of the CBC and the ATP synthase may affect the kinetics of photoinduced changes of the P_{700}^+ concentration. The theoretical curves presented in Fig. 3 were obtained at different values of the model parameters μ_1 and μ_2. The figure also shows a typical experimental curve of P_{700} photooxidation obtained earlier by the EPR method for *Tradescantia fluminensis* leaves [65]. The results of calculations indicate a relatively rapid growth of $[P_{700}^+]$ (stage *O–A*) immediately after switching on the light, followed by a decline of $[P_{700}^+]$ to an intermediate level *B*. Such a non-monotonic transition (*O–A–B*), characteristic of the first stages of the P_{700}^+ induction, is observed in experiments on measurements the kinetics of the P_{700} oxidation in leaves of higher plants using an optical method (see, for example, a detailed analysis of this phenomenon in the work of Bulychev and Vredenberg [52]). As it was shown earlier [44, 45], the height of the *O–A* peak depends on initial conditions: the peak is higher in the case of the initial oxidized plastoquinone pool than in the case of the reduced pool. The depth of *A–B* depends on the stoichiometry of PSII and PSI (data not shown), and the values of variable parameters μ_1 and μ_2, which reflect the degree of thioredoxin influence on the processes of the CBC and the ATP synthase activation. Figure 3 shows, as an example, the kinetic curves of the P_{700}^+ concentration computed for different values of $\mu_1 = \mu_2 \equiv \mu$. It is seen that at the initial stage of the induction process, the higher is the value of parameter μ, the higher the "plateau" level C is. This result can be explained by the fact that outflow of electrons from PSI at the initial stage of the induction period is the limiting step in the chain of noncyclic transport of electrons due to the low CBC activity. At the same time, the redundant reduction of the carriers at the acceptor site of PSI occurs due to the low rate of NADPH consumption. Therefore, the enhancement of the redox-dependent CBC activation, characterized by the parameter μ increase, promotes the growth of the P_{700}^+ concentration at the ini-

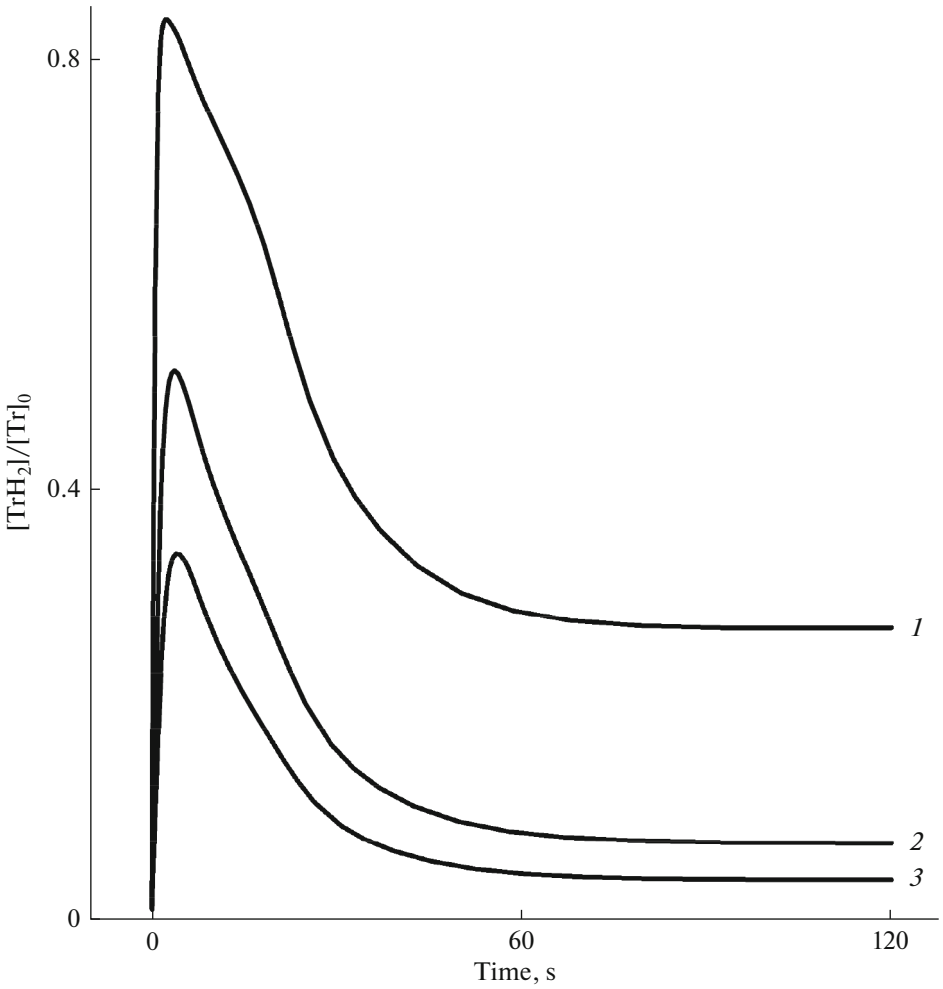

Fig. 2. The kinetics of thioredoxin reduction at various values of the parameter k_{FT}. Curve *1*, a high rate of thioredoxin reduction $k_{FT}/k^0_{FT} = 10$; curve *2*, a moderate rate $k_{FT}/k^0_{FT} = 5$; curve *3*, a low rate $k_{FT} = k^0_{FT}$.

tial stage of the induction process. Then, after a lag-phase, more intensive growth of $[P^+_{700}]$ occurs from level *C* to a stationary value *D*. The latter is because of two reasons: activation of the CBC reactions due to an increase in the stromal pH ($pH_o\uparrow$) and the attenuation of electron flow from PSII to PSI due to the pH decrease in the intrathylakoid space ($pH_i\downarrow$) (for details, see [43, 44]). When the rate of reduced thioredoxin interaction with the ATP synthase and the CBC enzymes increases, the lag phase prior to $[P^+_{700}]$ growth is shortened significantly, and the phase of slow $[P^+_{700}]$ growth (stage *C*–*D*) shifts to the left, indicating a marked acceleration of P_{700} photooxidation. Note that the accounting of the thioredoxin-dependent CBC activation allows a realistic description of the P_{700} photooxidation curve. As can be seen from Fig. 3, the experimental curve accurately falls into the "fork" between the two computed curves obtained for $\mu = 7$ and 10. Thus, the results of our simulations prove that thioredoxin-dependent activation of the CBC enzymes may exert a significant effect on the kinetics of the P_{700} photooxidation, because these processes influence the increase of the electron flows at the acceptor site of PSI.

The results of the simulation of the electron flows distribution of electron flows at the acceptor site of PSI during the induction period shown in Fig. 4 also demonstrate the influence of the thioredoxin-dependent activation of the CBC on the photosynthesis induction processes. On the acceptor side of PSI, the electron flux splits into three parts: a linear electron transport from Fd^- to $NADP^+$ and further into the CBC (curve J_{CBC}); cyclic transport via FQR, in which the electrons return to the ETC at the level of plastoquinone pool (curve J_{SC}), and the flow of electrons to oxygen (curve J_{O_2}). Changes in the electron fluxes and their ratio are determined by several factors: (i) the dependence of the PSII activity on the intrathylakoid pH_{in} and the stromal pH_{out}; (ii) activation of the CBC

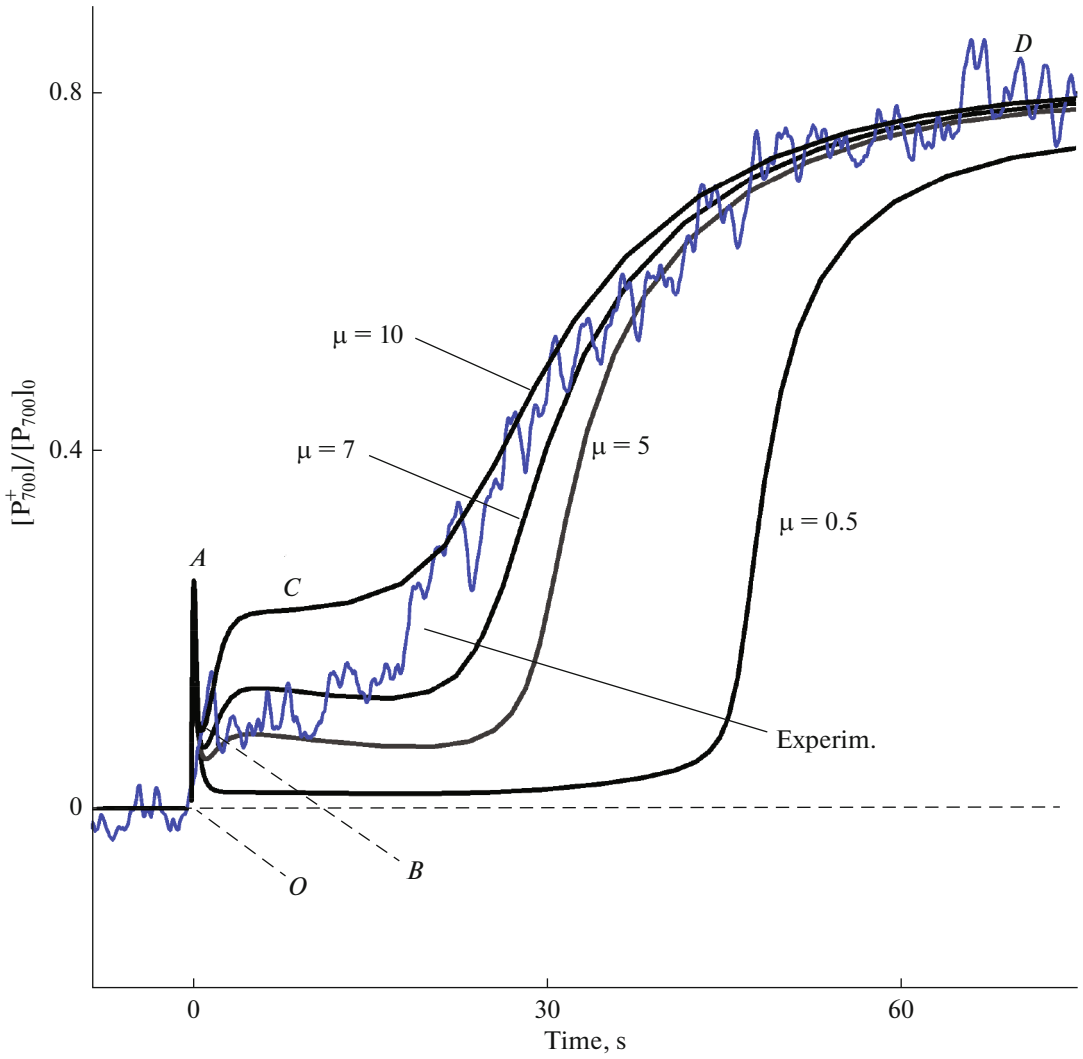

Fig. 3. The computed kinetics of photoinduced changes of the relative concentrations of oxidized reaction centers P^+_{700} in the chloroplasts at various parameters μ_1 and μ_2. The values of parameter $\mu = \mu_1 = \mu_2$ are indicated in the figure. The kinetic curve of photoinduced changes of the EPR signal from P^+_{700} of *Tradescantia fluminensis* leaves, which is a modified fragment of Fig. 8 from [65], is shown for comparison with the computed data.

enzymes as a result of the photoinduced alkalization of the stroma and the thioredoxin-dependent CBC regulation; (iii) the influence of pH_{in} on the rate of ATP synthesis, and (iv) activation of the ATP synthase by thioredoxin. It can be seen from Fig. 4a that at the initial moment of time, when the CBC is not active, the flow of electrons to $NADP^+$ is small (curve J_{CBC}) and the main flow of electrons from PSI is directed to the chain of the cyclic transport around PSI through FQR (curve J_{SC}). In these conditions, the flow of electrons to oxygen also occurs (the Mehler reaction, curve J_{O_2}). Over time, after ADP exhaustion (the system is in metabolic state 4), the J_{SC} and J_{O_2} flows weaken because of deceleration of electron transfer between PSII and PSI due to the acidification of the intrathylakoid space and also due to the diversion of electrons to the non-cyclic (linear) pathway of electron transfer in the CBC. In the stationary state, the electron flux to oxygen is not more than 10–15% of the flow to the CBC that corresponds to previously published data [46, 48]. For comparison, the kinetic curves shown in Figs. 4a and 4b were obtained for values of parameters μ_1 and μ_2 differing tenfold. The comparison of time dependencies for the three electron flows (J_{CBC}, the flow of electrons to the CBC; J_{SC}, the "short" cycle, and J_{O_2}, the flow of electrons to oxygen) shows that accounting of the processes of thioredoxin-dependent activation of the CBC and the ATP synthase enhances the main electron flow to the CBC (J_{CBC}) and is accompanied by some attenuation of the alternative flows J_{SC} and J_{O_2}. At the same time, as can be seen in Fig. 4b, the accounting of thioredoxin-dependent reg-

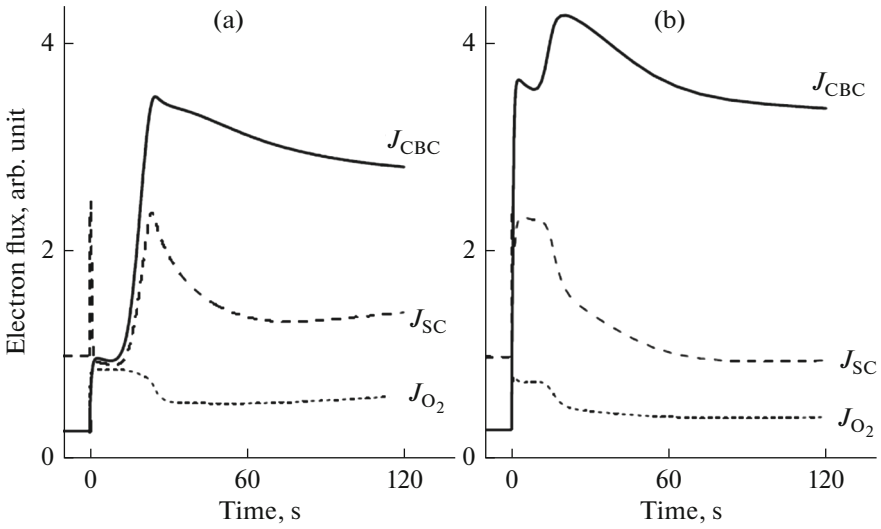

Fig. 4. The electron flows on the acceptor site of PSI in chloroplasts, in the conditions of redox-dependent activity regulation of the CBC and the ATP synthase by thioredoxin. (a) Slight activation of the thioredoxin-dependent CBC enzymes and the ATP synthase; (b) tenfold increase of the activation parameters μ_1 and μ_2. Curve J_{CBC}, the electron flux from NADPH in the CBC; curve J_{O_2}, the electron flux from ferredoxin to oxygen (Mehler reaction); curve J_{SC}, the electron flux from ferredoxin to quinone (the "short" cycle).

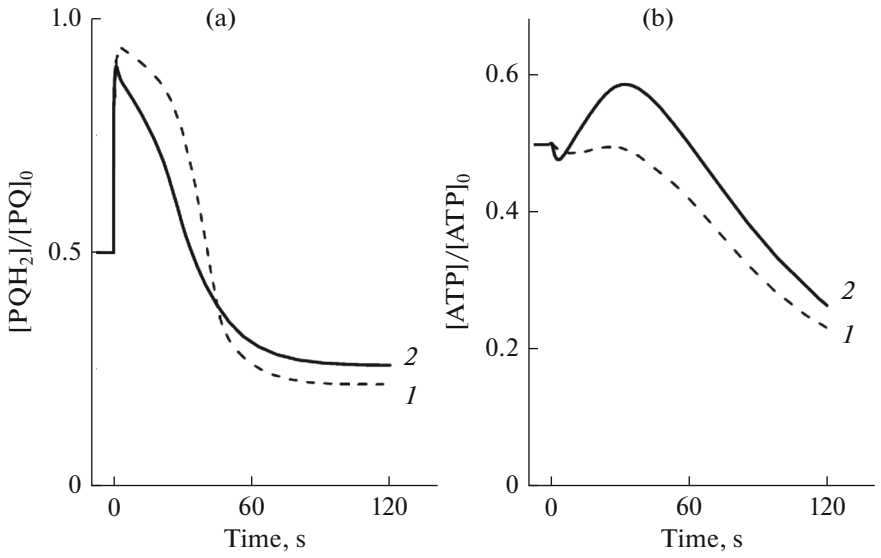

Fig. 5. The kinetics of photoinduced changes of the relative values of the variables $[PQH_2]$ (a) and [ATP] (b): curve *1*, a slight activation of the thioredoxin-dependent CBC enzymes and the ATP synthase; curve *2*, a tenfold increase of the activation parameters μ_1 and μ_2.

ulation leads to a noticeable reduction in the duration of the induction phase.

The computed kinetics of photoinduced redox transformations of plastoquinone and ATP concentration changes are shown presented in Fig. 5. Note that within the first 10 s after turning on the light, the plastoquinone pool becomes quickly reduced and then relatively slowly reoxidizes (within minutes), reaching the steady state level (Fig. 5a). A tenfold increase of parameters μ_1 and μ_2 produce some changes in the kinetic curves indicating acceleration of this process.

A different pattern is observed for the ATP concentration (Fig. 5b). The increase of the activation rate of the CBC enzymes and the ATP synthase by reduced thioredoxin leads to a pronounced non-monotonic dependence of ATP concentration on the time of illumination (Fig. 5b, curve *2*). Upon the activation of the ATP synthase, the intrathylakoid space is less acidified, as evidenced by the computed curves shown in

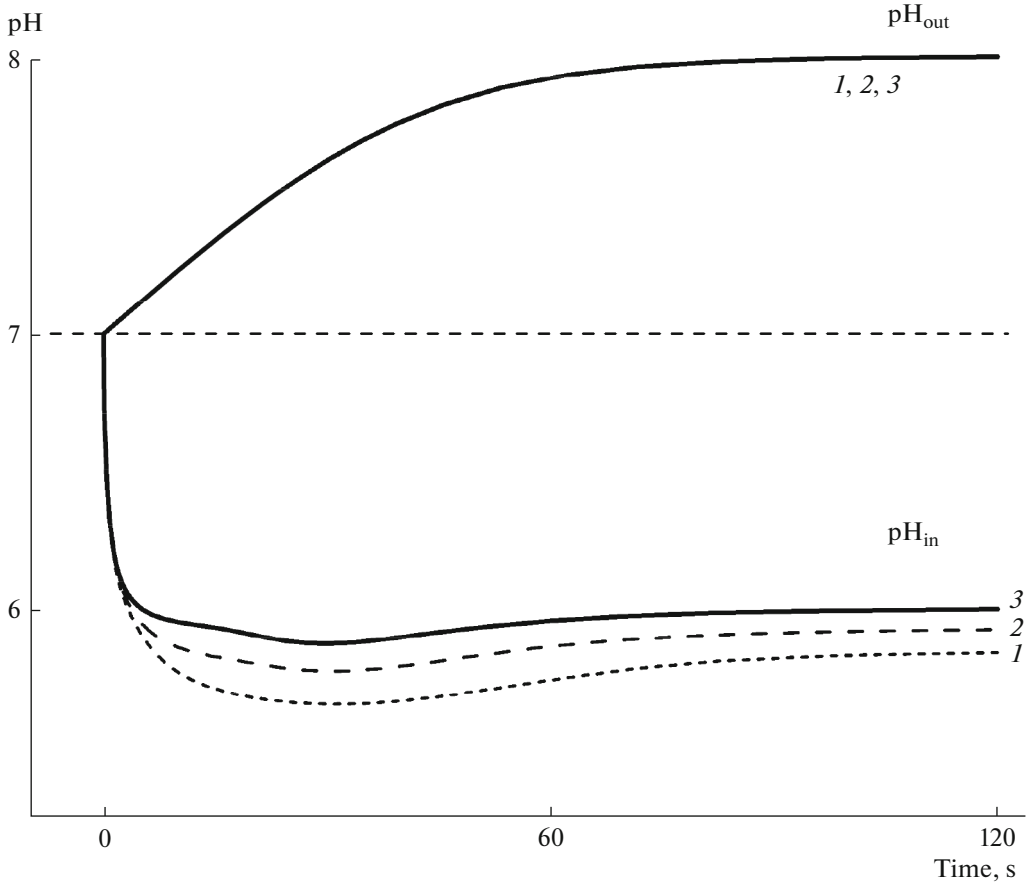

Fig. 6. The kinetics of photoinduced changes of intrathylakoid pH_i and pH_o in the stroma: curve *1*, a slight activation of the thioredoxin-dependent CBC enzymes and the ATP synthase; curve *2*, a 5-fold increase of the activation parameters μ_1 and μ_2; curve *3*, a tenfold increase of the activation parameters μ_1 and μ_2.

Fig. 6. It can also be seen in Fig. 6 that the non-monotonic dependence of intrathylakoid space acidification correlates with the course of the kinetic curves for ATP. Thus, the effects of the redox-dependent activation of the CBC and the ATP synthase relatively weakly affect the shape of the curves of pH_{in} changes, resulting in a slight increase by 0.2 units in the steady state pH_{in}. At the same time, as noted above, the P_{700}^+ induction kinetics and the proportion of alternative electron flows at the acceptor site of PSI are more sensitive to the processes of redox regulation.

CONCLUSIONS

Simulation of the electron transport processes, conducted within the previous mathematical model taking into account the pH-dependent regulation of the key stages of electron transport, made it possible to describe a number of patterns of complex kinetics of the electron transport processes in intact chloroplasts (see, e.g., review articles [37, 38]). In particular, it was shown that the multiphase kinetics of P_{700} photooxidation is determined by the change-over of the rate-limiting step: switching of electron fluxes on the acceptor side of PSI and the inhibition of electron transfer between PSII and PSI due to the acidification of the intrathylakoid space. The model plausibly describes the change of the metabolic state of chloroplasts caused by changes of the phosphate potential due the work of the membrane ATP synthase. At the same time, the mechanisms of photosynthesis regulation related to the redox-dependent activation of the CBC and the ATP synthase, mediated by the thioredoxin action, was not considered in the previous work. The results of the numerical experiments performed in this work allowed simulation of the impact of these factors on the kinetics of electron transport in native chloroplasts adapted to darkness.

The issue of verification of the comparatively complex kinetic model containing a large number of parameters requires comparison of the model predictions with experimental data. To this end, we compared the results of computations with the experimental data on P_{700}^+ induction in the higher plant leaves obtained by the EPR method. The advantage of EPR is that it allows direct recording of the status of the PSI

reaction centers (P_{700}) in chloroplasts in situ (leaves) by the magnitude of the characteristic signal from the oxidized P_{700}^+ centers [62]. The simulation of the redox transformations of P_{700} revealed a variety of kinetic patterns of the P_{700} photooxidation observed in the experiment [62]. It is known, for example, that the duration and quantitative relations between the phases of the kinetic curve of P_{700} oxidation may vary substantially, depending on the intensity and spectral composition of the acting light [38].

It was of interest to study how redox-dependent regulation of such key processes of photosynthesis as the ATP synthesis and the CBC functioning can manifest itself in the kinetics of P_{700} photooxidation. Comparison of the kinetic curves computed for various μ values showed that a relative contribution of the *B* phase increases and its duration decreases with increasing μ (Fig. 3). Low level of the P_{700}^+ signal recorded by different methods (EPR spectroscopy and optical methods) at the initial stage of induction is typically associated with slowed operation of the CBC and the increased contribution of cyclic electron flow, through which electrons are diverted from the acceptor site of PSI to P_{700}^+ [60, 66]. A realistic description of the multiphase kinetics of P_{700} photooxidation in leaves of higher plants was obtained by taking into account the redox-dependent activation of the CBC (μ = 7–10) (cf. theoretical curves with the experimental dependence shown in Fig. 3). As was noted above, the variation of the model parameters responsible for the activation of the ATP synthase affects the kinetics of P_{700} photooxidation to a lesser extent. The latter can be explained by the fact that the processes of the light-induced acidification of the intrathylakoid spaces are less sensitive to variation of the parameters related to the ATP synthase activation compared with the CBC.

Thus, the analysis of the results of the numerical experiments performed within the framework of the model developed has proved that, along with the regulation of the electron transfer between PSII and PSI (the attenuation of PSII activity due to non-photochemical quenching of chlorophyll excitation in the light-harvesting antenna of PSII, slowing PQH_2 oxidation by the cytochrome b_6f complex and alkalization of the narrow gap between adjacent thylakoids of granum), thioredoxin-dependent activation of the CBC enzymes also affects the induction processes and the distribution of electron fluxes on the acceptor side of PSI. Hopefully, further development of the model aimed at scrutinizing the processes of the electron transfer in PSII and PSI will allow extension of the model applicability to the description of the chloroplast interactions with other metabolic systems of the plant cell, including the interaction of chloroplasts with mitochondria through common metabolites of carbon and nitrogen metabolism. The creation of adequate models of photosynthesis will ensure the development of a reliable and efficient tool for in-depth analysis of light-dependent energy conversion in nature in a wide range of times, from fractions of seconds to tens of minutes.

APPENDIX

To describe the electron transport processes, a system of ordinary differential equations has been considered describing the behavior of the following variables: $[P_{700}^+]$ is the concentration of the oxidized centers of P_{700} (primary electron donor in PSI), $[P_{680}^+]$ is the concentration of the oxidized centers of P_{680} (primary electron donor in PSII), [Pc] is the concentration of the oxidized carriers which are the immediate electron donors for the oxidized centers of P_{700} (plastocyanin and/or cytochrome c_6), [PQ] is the concentration of oxidized plastoquinone, $[Fd^+]$ is the concentration of oxidized ferredoxin, $[N^+]$ and [NH] is the concentration of $NADP^+$ and NADPH, the terminal electron acceptors of PSI in the oxidized and reduced forms, respectively, $[O_2]$ is oxygen concentration in the medium. The variable [ATP] describes changes in the concentration of ATP.

The initial system of equations, describing the behavior of the electron carriers, the change in the concentration of protons inside the thylakoid $[H_i^+]$ and in the stroma $[H_o^+]$, the processes of emission and consumption of molecular oxygen and the change in the concentration of ATP, which accounts for thioredoxin-dependent activation of the CBC and the ATP synthase, was described previously [42–45]. This system has the following form:

$$\frac{d[\mathrm{ATP}]}{dt} = \omega_1([\mathrm{ADN}]-[\mathrm{ATP}])J_{\mathrm{ATP}}(t) - k_{\mathrm{CBC}}\omega_2([\mathrm{NH}],[\mathrm{ATP}]), \quad \text{(S1)}$$

$$\frac{d[\mathrm{NH}]}{dt} = k_{\mathrm{NH}}[H_o^+]([N_0]-[N^+]-[\mathrm{NH}]) - k_{N^-}[\mathrm{NH}] - k_{\mathrm{NQ}}[H_o^+][\mathrm{PQ}][\mathrm{NH}] - k_{\mathrm{CC}}([\mathrm{NH}],[\mathrm{ATP}]), \quad \text{(S2)}$$

$$\frac{d[N^+]}{dt} = k_{\mathrm{CC}}([\mathrm{NH}],[\mathrm{ATP}]) - [N^+]\left\{0.5k_{\mathrm{FN}}\left([\mathrm{Fd}]_0-[\mathrm{Fd}^+]\right)+k_{\mathrm{RC}}\right\} + k_{\mathrm{NQ}}[H_o^+][Q][\mathrm{NH}], \quad \text{(S3)}$$

$$\frac{d[\mathrm{Fd}^+]}{dt} = \left\{k_{\mathrm{FQ}}[H_o^+][\mathrm{PQ}]+k_{\mathrm{FN}}[N^+]+k_{\mathrm{FO}}[O_2]\right\} \times \left([\mathrm{Fd}]_0-[\mathrm{Fd}^+]\right) - L_1k_{\mathrm{P700}}[\mathrm{Fd}^+]\left([P_{700}]_0-[P_{700}^+]\right), \quad \text{(S4)}$$

$$\frac{d[O_2]}{dt} = 0.25k_{H_2O}[P_{680}^+] - [O_2] \times \{k_{OX1}([PQ]_0 - [PQ]) + k_{OX2}([Pc]_0 - [Pc]) + 0.5k_{FO}([Fd]_0 - [Fd^+])\}, \quad (S5)$$

$$\frac{d[P_{680}^+]}{dt} = L_2([H_i^+])k_{P680}[H_o^+][PQ] \times ([P_{680}]_0 - [P_{680}^+]) - k_{H_2O}[P_{680}^+], \quad (S6)$$

$$\frac{d[P_{700}^+]}{dt} = L_1k_{P700}[Fd^+]([P_{700}]_0 - [P_{700}^+]) - k_{Pc}[P_{700}^+]([Pc]_0 - [Pc]), \quad (S7)$$

$$\frac{d[Pc]}{dt} = k_{OX_2}([Pc]_0 - [Pc])[O_2] + k_{Pc}[P_{700}^+]([Pc]_0 - [Pc]) - \sigma_{bf}k_Q([PQ],[Pc],[H_i^+]), \quad (S8)$$

$$\frac{d[PQ]}{dt} = 0.5\sigma_{bf}k_Q([PQ],[Pc],[H_i^+]) + 0.5k_{OX_1}([PQ]_0 - [PQ])[O_2] - [PQ][H_o^+]\{k_{NQ}[NH] + 0.5k_{FQ}([Fd]_0 - [Fd^+]) + 0.5L_2([H_i^+])k_{P680}([P_{680}]_0 - [P_{680}^+])\}, \quad (S9)$$

$$\left[1 + \frac{K_oB_o}{(K_o + [H_o^+])^2}\right]\frac{d[H_o^+]}{dt} = -\frac{2}{l_o}\begin{Bmatrix} [PQ][H_o^+]\{k_{NQ}[NH] + k_{FQ}([Fd]_0 - [Fd^+]) + L_2k_{P680}([P_{680}]_0 - [P_{680}^+])\} \\ + k_{NH}[H_o^+]([N_0] - [N^+] - [NH]) - k_{N^-}[NH] + k_{FO}[O_2]([Fd]_0 - [Fd^+]) \\ + k_{CC}([NH],[ATP]) + J_{cell}(t) - J_{pass}(t) - ([ADN] - [ATP])J_{ATP}(t) \end{Bmatrix}, \quad (S10)$$

$$\left[1 + \frac{K_iB_i}{(K_i + [H_i^+])^2}\right]\frac{d[H_i^+]}{dt} = \frac{2}{l_i}\begin{Bmatrix} k_{H_2O}[P_{680}^+] + 2\sigma_{bf}k_Q([PQ],[Pc],[H_i^+]) \\ -J_{pass}(t) - ([ADN] - [ATP])J_{ATP}(t) \end{Bmatrix}. \quad (S11)$$

Constants ω_1 and ω_2 express the stoichiometry of proton transfer through the ATP synthase and consumption of ATP and final electron acceptor NADPH in the reactions of the Calvin cycle and are equal to 14/3 and 3/2, respectively. The parameter L_1 and the function L_2 (pH_i) describe the number of quanta of light falling per unit time upon the reduced reaction centers of P_{700} and P_{680}, respectively. Constants marked with a subscript "0" are the maximal concentrations of the relevant variables. $[N]_0$ and [ADN] are the total concentrations of all forms of NADP and adenine nucleotides, respectively. Constant σ_{bf} is the surface density of the b_6/f complexes in the membrane; k_{H_2O}, k_{P680}, k_Q, k_{Pc}, k_{P700}, k_{FQ}, k_{FO}, k_{FN}, k_{NH}, k_{N^-}, k_{CC} and k_{NQ} are the effective rate constants of the reactions shown in Fig. 1. k_{RC} is the effective rate constant of the $NADP^+$ reduction due to nonphotosynthetic metabolic processes (for example, due to pentosophosphate pathway of glucose oxidation [1]). The set of model parameters K_i, K_o and B_i, B_o characterizes the buffer properties of the system. Here, K_i and K_o are the equilibrium constants for the reaction of proton binding by buffer groups inside and outside of the thylakoid membrane, respectively; Bi and Bo are the concentrations of these buffer groups (for details, see [54]). The model parameters l_i and l_o characterize the thickness of the lumen and the distance between the thylakoids of the stroma.

Plastoquinone oxidation and consequent intrathylakoid space acidification can be produced not only by the b_6/f complex, but also by the terminal oxidase of the *bd* type. Cytochrome c_6 can serve as the primary electron donor for both PSI and the cytochrome oxidase of aa_3 type. The constants k_{OX1} and k_{OX2} characterize the activity of the respective terminal oxidases of *bd* and aa_3 type. In addition, it is assumed that PSI can donate electrons to molecular oxygen.

The values of the rate constants, which characterize different stages of the electron transfer along the ETC from the water splitting complex of PSII to various PSI acceptors, were chosen on the basis of the published data on the kinetics of partial reactions of electron transport in different segments of the chloroplast ETC. The characteristic times of intermediate redox electron transfer reactions in the photosynthetic electron transport chain are given in Table 1S.

The chosen rate constants of electron-transport processes, as can be seen from Table 1S, are in the ranges of characteristic times obtained experimentally. To refine the constants used in the model, the results of computations were compared with the experimental data obtained for various photosynthetic systems of oxygenic type (chloroplasts of higher plants and cyanobacteria) (see [37] for details). As a criterion of adequacy of the choice of rate constants, the agreement has been used of the theoretical curves with the experimental data of the electron transfer rate between PSII and PSI, as well as the intrathylakoid space pH (pH_i)

Table 1S. Characteristic times of intermediate redox electron transfer reactions in the photosynthetic electron transport chain

Electron transfer reaction	Rate constant	Characteristic time, $\tau_{1/2}$, s		References on experim. data
		model	experiment	
$H_2O \rightarrow P_{680}$	k_{H_2O}	10^{-4}	10^{-6}–6×10^{-4}	[57, 67]
$P_{680} \rightarrow PQ$	k_{P680}	6×10^{-4}	6×10^{-4}	[57, 67]
$Pc \rightarrow P_{700}$	k_{Pc}	2×10^{-4}	2×10^{-4}	[57, 67]
$P_{700} \rightarrow Fd$	k_{P700}	10^{-4}	10^{-2} –7×10^{-1}	[57, 67]
$Fd \rightarrow NADP$	k_{FN}, k_{NH}	10^{-2}	2×10^{-4} –10^{-2}	[68]
$Fd \rightarrow PQ$	k_{FQ}	2×10^{-2}	10^{-2} –7×10^{-1}	[60]
$Fd \rightarrow O_2$	k_{O_2}	9×10^{-2}	2×10^{-2} –7×10^{-1}	[47]

and pH of the stroma (pH_o) at metabolic states 3 (the conditions of intensive ATP synthesis) and 4 (the state of photosynthetic control). It was accepted, in particular, that at metabolic states 3 and 4 $pH_i \approx 6.0$–6.2 and $pH_i \approx 5.4$–5.6, respectively [19, 59].

Derivation of the equation for the passive flow J_{pass} was based on the assumption about the participation of acidic groups of the thylakoid membrane in the processes of transmembrane transfer of protons as mediators. There are indications in the literature that, at physiological pH, the conductivity of lipid bilayer is determined mainly by the presence of acidic groups in the membranes [71–73]. The model of "acidic" carrier was used to describe the passive leakage of protons in thylakoids; it has been shown that it gives good agreement with the experimental data on measurements of the photoinduced uptake of protons by the chloroplasts [61]. According to the model considered in [61], a proton inside the thylakoid first binds to an intramembrane proton-acceptor group M ($H^+_{in} + M \leftrightarrow MH^+$), and then dissociates into the stroma ($MH^+ \leftrightarrow M + H^+_{out}$). The binding of hydrogen ions H^+ inside the thylakoid to the proton-acceptor groups M is characterized by an effective rate constant k_1'; the binding of hydrogen ions taken from the external space is characterized by an effective rate constant k_2'. The dissociation of protons into the thylakoid and out of it is characterized by effective rate constants k_{-1}' and k_{-2}', respectively. The rate constants of the direct and reverse reactions are related by the ratio $k_1'/k_{-1}' = K_{M1}$ and $k_2'/k_{-2}' = K_{M2}$, where K_{M1} and K_{M2} are the effective constants of the proton equilibrium for the buffer group M and hydrogen ions inside and outside of the thylakoid, respectively. It is reasonable to assume that, for the proton-acceptor groups M, fixed in the membrane and involved in the passive transfer of protons across the membrane, equality $K_{M1} = K_{M2} \equiv K_M$ must be true. It is easy to show (for details, see [61]) that the function J_{pass}, describing the passive proton flow in the framework of the model, schematically shown in Fig. 1 on the left, is as follows:

$$J_{pass}(t) = \frac{k_{-2}'\left([H_i(t)] - [H_o(t)]\right)}{10^{-pK_M}\left(1 + k_2'/k_1'\right) + \left([H_i(t)] + [H_o(t)]\right)k_2'/k_1'}. \quad \text{(S12)}$$

It is obvious that the equation for the proton flow through the ATP synthase, J_{ATP}, in general case, may be different from Eq. (S12), since the transmembrane proton transport, associated with ATP synthesis, has additional stages due to the structural features of the ATP synthase complex. The justification of the choice of a function J_{ATP} for the ATP synthase channel of the transmembrane proton transfer and a function J_{cell} of the exchange of protons between the stroma and the cytosol was given in [37]. Note that specific values of the constants in the formulas for the proton flows J_{ATP} and J_{pass} have been chosen by fitting the experimental data so that to obtain the best agreement of the computed and experimental values of pH_i and the rate of ATP synthesis at different pH_o.

The function $k_{PQ}\{[PQ],[Pc],[H_i]\} = 1/\tau_{PQ}$, where

$$\tau_{PQ} = \frac{1}{k_z([PQ]_0 - [PQ])} + T_1[H_i^+]/h_1 + T_2[H_i^+]/h_2 + T_3 + \frac{1}{2k_y[Pc]}, \quad \text{(S13)}$$

was determined earlier [54]. This function is an effective rate constant, which characterizes the set of processes associated with the oxidation of the plastoquinone molecule PQH_2 dependent on the intrathylakoid pH_{in}. Here, k_z is the binding constant of PQH_2 to the Q_o center of the cytochrome b_6f complex, T_i ($i = 1, 2, 3$) are the characteristic times of transfer of two electrons from the bound PQH_2 molecule to the b_6f complex and electron transfer within this complex, respectively; k_y is the rate constant of electron transfer to the oxidized Pc molecule. The characteristic time of the plastoquinone oxidation, τ_{PQ}, is determined by the

rate of its direct interaction with the cytochrome b_6f complex and the transfer time of an electron from the b_6f complex to plastocyanin. The rate of PQH_2 oxidation depends on the concentration of hydrogen ions inside the thylakoids (for details, see [38, 39]). The parameters h_1 and h_2 are normalizing coefficients, the magnitudes of which are determined by pK of the first and second stages the of PQH_2 oxidation.

For the simulation of non-photochemical quenching, the constant L_2, which characterizes a number of light quanta exciting P_{680} per unit time, was phenomenologically given as L_2 (pH_i) function, parametrically depending on pH_i. By this means we took into account that, during the acidification of the lumen, photochemical activity of PSII is reduced. The function L_2 (pH_i) has the following form:

$$L_2(\mathrm{pH_i}) = \begin{cases} (L_0/2)\left[(1-L_{\min})[2-e^{-k[\mathrm{pH_i}-\mathrm{p}K]}]+2L_{\min}\right] & \mathrm{pH_i} > \mathrm{p}K \\ (L_0/2)[(1-L_{\min})e^{k[\mathrm{pH_i}-\mathrm{p}K]}+2L_{\min}] & \mathrm{pH_i} \le \mathrm{p}K \end{cases}. \quad \text{(S14)}$$

Constants k, L_0 and $L_{\min}$, are the model parameters. pK characterizes the activation of non-photochemical quenching of chlorophyll excitation in the light-harvesting antenna of PSII. The dependence of $L_2(pH_i)$ on pH_i has a sigmoidal form, describing the L_2 decrease in the range from pH 8 (where $L_2 = L_0$) to pH 4 (where $L_2 = L_0L_{\min}$).

The NADP and ATP consumption in the Calvin–Benson cycle is described in a generalized form by a function proposed earlier [44]:

$$k_{\mathrm{CBC}}([\mathrm{NH}],[\mathrm{ATP}]) = \left(\frac{k^s_{\min}-k^s_{\max}}{1+\exp\left\{\frac{\mathrm{pH_o}-X_0}{\Delta X}\right\}}+k^s_{\max}\right) \times \left(\frac{[\mathrm{ATP}][\mathrm{NH}]}{k^s_2+k^s_3[\mathrm{ATP}]+k^s_4[\mathrm{NH}]+k^s_5[\mathrm{ATP}][\mathrm{NH}]}\right). \quad \text{(S15)}$$

The first factor in Eq. (15) is the Boltzmann function, phenomenologically describing the pH-dependent activation of the Calvin–Benson cycle enzymes due to the photoinduced stroma alkalizing. It has been chosen according to the literature data on the dependence of activity of some Calvin cycle enzymes on pH of the stroma [1, 5].

Numerical integration of the system of differential equations was performed by the Runge–Kutta method.

ACKNOWLEDGMENTS

The work was partially supported by the Russian Foundation for Basic Research (project nos. 15-04-03790 and 18-04-00214).

REFERENCES

1. Edwards G.E., Walker D.A. 1983. *C3, C4: Mechanisms, and cellular and environmental regulation of photosynthesis.* Blackwell, Oxford.
2. Blankenship R.E. 2002. *Molecular mechanisms of photosynthesis.* Malden, MA: Blackwell Science Inc.
3. Nelson N., Yocum C.F., 2006. Structure and function of photosystems I and II. *Annu. Rev. Plant. Biol.* **57**, 521–565.
4. Skulachev V.P., Bogachev A.V., Kasparinsky F.O. 2012. *Principles of Bioenergetics.* Springer.
5. Nelson D.L., Cox M.M. 2012. *Lehninger principles of biochemistry.* 6th edn. New York: Freeman W. H. & Company.
6. Mamedov M., Govindjee, Nadtochenko V., Semenov A. 2015. Primary electron transfer processes in photosynthetic reaction centers from oxygenic organisms. *Photosynth. Res.* **125**, 51–63.
7. Nelson N., Junge W. 2015. Structure and energy transfer in photosystems of oxygenic photosynthesis. *Annu. Rev. Biochem.* **84**, 659–683.
8. Junge W., Nelson N. 2015. ATP synthase. *Annu Rev Biochem.* **83**, 631–657.
9. Romanovsky Yu.M., Tikhonov A.N. 2010. Molecular energy transducers of the living cell. Proton ATP synthase: A rotating molecular motor. *Physics Uspekhi.* **53** (9), 893–914.
10. Anderson J.M. 1982. Distribution of the cytochromes of spinach chloroplasts between the appressed membranes of grana stacks and stroma-exposed thylakoid regions. *FEBS Lett.* **138**, 62–66.
11. Albertsson P.-A. 2001. A quantitative model of the domain structure of the photosynthetic membrane. *Trends Plant Sci.* **6**, 349–354.
12. Staehelin L.A. 2003. Chloroplast structure: From chlorophyll granules to supra-molecular architecture of thylakoid membranes. *Photosynth. Res.* **76**, 185–196.
13. Dekker J.P., Boekema E.J. 2005. Supramolecular organization of thylakoid membrane proteins in green plants. *Biochim. Biophys. Acta.* **1706**, 12–39.
14. Daum B., Kuhlbrandt W. 2011. Electron tomography of plant thylakoid membranes. *J. Exp. Bot.* **62,** 2393–2402.
15. Kirchhoff H. 2013. Architectural switches in plant thylakoid membranes. *Photosynth. Res.* **116,** 481–487.
16. Kirchhoff H. 2014. Diffusion of molecules and macromolecules in thylakoid membranes. *Biochim. Biophys. Acta.* **1837**, 495–502.
17. Kirchhoff H., Hall C., Wood M., Herbstova M., Tsabari O., Nevo R., Charuvi D., Shimoni E., Reich Z. 2011. Dynamic control of protein diffusion within the

granal thylakoid lumen. *Proc. Natl. Acad. Sci. USA.* **108**, 20248–20253.

18. Buchanan B.B. 1991. Regulation of CO_2 assimilation in oxygenic photosynthesis: The ferredoxin/thioredoxin system. Perspective on its discovery, present status, and future development. *Arch. Biochem. Biophys.* **288**, 1–9.
19. Tikhonov A.N. 2013. pH-Dependent regulation of electron transport and ATP synthesis in chloroplasts. *Photosynth. Res.* **116**, 511–534.
20. Puthiyaveetil S., Kirchhoff H., Höhner R. 2016. Structural and functional dynamics of the thylakoid membrane system. In: *Chloroplasts. Current research and future trends.* Kirchhoff H., ed., Norfolk, UK: Caister Academic Press, pp. 59–87.
21. Balsera M., Schumann P., Buchanan B.B. 2016. Redox regulation in chloroplasts. In: *Chloroplasts. Current research and future trends.* Kirchhoff H., ed., Norfolk, UK: Caister Academic Press, pp. 187–207.
22. Mills J.D., Mitchell P. 1984. Thiol modulation of the chloroplast ATPase and its effect on photophosphorylation. *Biochim. Biophys. Acta.* **764**, 93–104.
23. Balmer Y., Koller A., del Val G., Manieri W., Schürmann P., Buckanan B.B. 2003. Proteomics gives insight into the regulatory function of chloroplast thioredoxins. *Proc. Natl. Acad. Sci. USA,* **100**, 370–375.
24. Dietz K.-J., Pfannschmidt T., 2011. Novel regulators in photosynthetic redox control of plant metabolism and gene expression. *Plant Physiol.* **155**, 1477–1485.
25. Michelet L., Zaffagnini M., Morisse S., Sparla F., Pérez-Pérez M.E., Francia F., Danon A., Marchand C.H., Fermani S., Trost P., Lemaire S.D. 2013. Redox regulation of the Calvin–Benson cycle: Something old, something new. *Front. Plant Sci.* **4**, http://dx.doi.org/, Article 470.10.3389/fpls.2013.00470.
26. Kramer D.M., Avenson T.J., Edwards G.E. 2004. Dynamic flexibility in the light reactions of photosynthesis governed by both electron and proton transfer reactions. *Trends Plant Sci.* **9**, 349–357.
27. Eberhard S., Finazzi G., Wollman F.A. 2008. The dynamics of photosynthesis. *Annu. Rev. Genet.* **42**, 463–515.
28. Niyogi K.K., Truong T.B. 2013. Evolution of flexible non-photochemical quenching mechanisms that regulate light harvesting in oxygenic photosynthesis. *Curr. Opin. Plant Biol.* **16**, 307–14.
29. Maslakov A.S., Antal T.K., Riznichenko G.Yu., Rubin A.B. 2016. Modeling of primary photosynthetic processes by using kinetic method of Monte Carlo. *Biofizika* (Rus.). **61**, 464–477.
30. Kukushkin A.K., Tikhonov A.N. 1988. *Lektsii po biofizike fotosintza visshih rasteniy.* (Lectures on biophysics of photosynthesis in higher plants). M.: Moscow State University.
31. *Photosynthesis in silico: Understanding complexity from molecules to ecosystems.* 2009. Laisk A., Nedbal L., Govindjee., eds. Dordrecht: Springer.
32. Rubin A., Riznichenko G. 2014. *Mathematical Biophysics.* Series: Biological and medical physics, biomedical engineering, XV. New York, Heidelberg, Dordrecht, London: Springer, pp. 141–247. doi 10.1007/978-1-4614-8702-9
33. Tikhonov A.N. 2016. Modeling electron and proton transport in chloroplasts. In: *Chloroplasts. Current research and future trends.* Kirchhoff H., ed., Norfolk, UK: Caister Academic Press, pp. 101–134.
34. Vershubskii A.V. Priklonskii V.I., Tikhonov A.N. 2001. Electron and proton transport in chloroplasts: A mathematical model constructed with regard for the lateral heterogeneity of thylakoids. *Biophysics.* **58**, 448–457.
35. Vershubskii A.V. Priklonskii V.I., Tikhonov A.N. 2003. A mathematical model of diffusion-controlled processes of electron and proton transport in chloroplasts with non-uniform distribution of photosystems I and II in thylakoids. *Biol. Membrany* (Rus.). **20**, 184–192.
36. Vershubskii A.V. Priklonskii V.I., Tikhonov A.N. 2004. The influence of diffusion and topological factors on the efficiency of energy coupling in chloroplasts with inhomogeneous lateral distribution of protein complexes in grans and intergran thylakoids. Mathematical modeling. *Biochemistry* (Moscow). **69**, 1016–1024.
37. Vershubskii A.V., Kuvykin I.V., Priklonsky V.I., Tikhonov A.N. 2011. Functional and topological aspects of pH-dependent regulation of electron and proton transport in chloroplasts *in silico. Biosystems.* **103**, 164–179.
38. Tikhonov A.N., Vershubskii A.V. 2014. Computer modeling of electron and proton transport in chloroplasts. *Biosystems.* **121**, 1–21.
39. Vershubskii A.V., Trubitsin B.V., Priklonskii V.I., Tikhonov A.N. 2017. Lateral heterogeneity of the proton potential along the thylakoid membranes of chloroplasts. *Biochim. Biophys. Acta.* **1859**, 388–401.
40. Heldt H.W., Werdan K., Milivancev M., Geller G. 1973. Alkalization of the chloroplast stroma caused by light-dependent proton flow into the thylakoid space. *Biochim. Biophis. Acta* **314**, 224–241.
41. Robinson S.P. 1985. The involvement of stromal ATP in maintaining the pH gradient across the chloroplast envelope in the light. *Biochim. Biophis. Acta.* **806**, 187–194.
42. Vershubskii A.V. Priklonskii V.I., Tikhonov A.N. 2004. Mathematical modeling of electron and proton transport coupled with ATP synthesis in chloroplasts. *Biophysics.* **49**, 52–65.
43. Kuvykin I.V., Vershubskii A.V., Tikhonov A.N. 2009. Alternative pathways of photoinduced electron transport in chloroplasts. *Russ. J. Phys. Chem. B.* **3**, 230–241.
44. Vershubskii A.V., Tikhonov A.N. 2013. Electron transport and transmembrane proton transfer in photosynthetic systems of oxygenic type *in silico. Biophysics.* **58**, 60–71.
45. Vershubskii A.V., Mishanin V.I., Tikhonov A.N. 2014. Modeling of the photosynthetic electron transport regulation in cyanobacteria. *Biochemistry (Moscow) Supplement Series A: Membrane and Cell Biology.* **8**, 262–278.
46. Heber U. 2002. Irrungen, wirrungen? The Mehler reaction in relation to cyclic electron transport in C_3 plants. *Photosynth. Res.* **73**, 223–231.
47. Kuvykin I.V., Vershubskii A.V., Ptushenko V.V., Tikhonov A.N. 2008. Oxygen as an alternative electron acceptor in the photosynthetic electron transport chain of C_3 plants. *Biochemistry (Moscow).* **73**, 1063–1075.

48. Ort D.R., Baker N.R. 2002. A photoprotective role for O_2 as an alternative electron sink in photosynthesis? *Curr. Opp. Plant Biol*. **5**, 193–197.
49. Egorova E.A., Bukhov N.G. 2006. Mechanisms and functions of photosystem I-related alternative electron transport pathways in chloroplasts. *Russ. J. Plant Physiol*. **53**, 571–582.
50. Burrows P.A., Sazanov L.A., Svab Z., Maliga P., Nixon P.J. 1998. Identification of a functional respiratory complex in chloroplasts through analysis of tobacco mutants containing disrupted plastid ndh genes. *EMBO J*. **17**, 868–876.
51. Peltier G., Cournac L. 2002. Chlororespiration. *Annu. Rev. Plant Biol*. **53**, 523–550.
52. Bulychev A.A., Vredenberg A.A. 2010. Induction kinetics of photosystem I-activated P_{700} oxidation in plant leaves and their dependence on pre-energization. *Russ. J. Plant Physiol*. **57**, 599-608.
53. Tikhonov A.N. 2012. Energetic and regulatory role of proton potential in chloroplasts. *Biochemistry (Moscow)*. **77**, 956–974.
54. Dubinsky A.Yu., Tikhonov A.N. 1997. A mathematical model of the thylakoid as a distributed heterogeneous system of electron and proton transport. *Biofizika* (Rus.). **42**, 644–661.
55. Turina P., Petersen J., Graber P. 2016. Thermodynamics of proton transport coupled ATP synthesis. *Biochim. Biophys. Acta*. **1857**, 653–664.
56. Hisabori T., Konno H., Ichimura H., Strotmann H., Bald D. 2002. Molecular devices of chloroplast F_1-ATP synthase for regulation. *Biochim. Biophys. Acta*. **1555**, 140–146.
57. Haehnel W. 1984. Photosynthetic electron transport in higher plants. *Annu. Rev. Plant Physiol. Plant Mol. Biol*. **35**, 659–693.
58. Tikhonov A.N. 2014. The cytochrome b_6f complex at the crossroad of photosynthetic electron transport pathways. *Plant Physiol. Biochem*. **81**, 163–183.
59. Kramer D.M., Sacksteder C.A., Cruz J.A. 1999. How acidic is the lumen? *Photosynth. Res*. **60**, 151–163.
60. Joliot P., Joliot A. 2005. Quantification of cyclic and linear flows in plants. *Proc. Natl. Acad. Sci. USA*. **102**, 4913–4918.
61. Dubinsky A.Yu., Tikhonov A.N. 1995. Mathematical modeling of photoinduced proton absorption by chloroplasts for various mechanisms of the leak of protons through the thylakoid membrane. *Biofizika* (Rus.). **40**, 365–371.
62. Tikhonov A.N. 2015. Induction events and short-term regulation of electron transport in chloroplasts: An overview. *Photosynth. Res*. **125**, 65–94.
63. Schreiber U., Klughammer C. 2016. Analysis of photosystem I donor and acceptor sides with a new type of online deconvoluting kinetic LED-array spectrophotometer. *Plant Cell Physiol*. **57**, 1454–1467.
64. Schreiber U. 2017. Redox changes of ferredoxin, P_{700}, and plastocyanin measured simultaneously in intact leaves. *Photosynth. Res*. **134**, 343–360.
65. Mishanin V.I., Trubitsin B.V., Benkov M.A., Minin A.A., Tikhonov A.N. 2016. Light acclimation of shade-tolerant and light-resistant *Tradescantia* species: Induction of chlorophyll a fluorescence and P_{700} photooxidation, expression of *PsbS* and *Lhcb*1 proteins. *Photosynth. Res*. **130**, 275–291.
66. Joliot P., Joliot A. 2006. Cyclic electron flow in C_3 plants. *Biochim. Biophys. Acta*. **1757**, 362–368.
67. Witt H.T. 1979. Energy conversion in the functional membrane of photosynthesis. Analysis by light pulse and electric pulse methods. *Biochim. Biophys. Acta*. **505**, 355–427.
68. Medina M., Gomes-Moreno C. 2004. Interaction of ferredoxin-$NADP^+$ reductase with its substrates: optimal interaction for efficient electron transfer. *Photosynth. Res*. **79**, 113–131.
69. Kuvykin I.V., Ptushenko V.V., Vershoubsky A.V., Tikhonov A.N. 2011. Regulation of electron transport in C_3 plant chloroplasts in situ and in silico. Short-term effects of atmospheric CO_2 and O_2. *Biochim. Biophys. Acta*. **1807**, 336–347.
70. Kanazawa A., Kramer D.M. 2002. In vivo modulation of non-photochemical exciton quenching (NPQ) by regulation of the chloroplast ATP synthase. *Proc. Natl. Acad. Sci. USA*. **99,** 12789–12794.
71. Nagle J.F. 1987. Theory of passive proton conductance in lipid bilayers. *J. Bioenerg. Biomembr*. **19,** 413–426.
72. Gutknecht J. 1987. Weak electrolyte transport across biological membranes. General principles. *J. Bioenerg. Biomembr*. **19**, 427–455.
73. Deamer D.W. 1987. Proton permeation of lipid bilayers *J. Bioenerg. Biomembr*. **19**, 457–479.

Translated by E. Puchkov